



Study of mineralogy and leaching behavior of stabilized/solidified sludge using differential acid neutralization analysis

Part II: Use of numerical simulation as an aid tool for cementitious hydrates identification

O. Peyronnard ^{a,*}, D. Blanc ^a, M. Benzaazoua ^b, P. Moszkowicz ^a

^a LGCIE Site Carnot, INSA-Lyon, 9 rue de la Physique, Villeurbanne, F 69621, France

^b UQAT, 445 Blvd de l'Université, Rouyn-Noranda, Québec, Canada J9X 5E4

ARTICLE INFO

Article history:

Received 29 October 2007

Accepted 27 March 2009

Keywords:

Waste management (E)

Modeling (E)

Mineral assemblage

Fly ash (D)

Portland cement (D)

ABSTRACT

In this work, we propose a methodology coupling differential acid neutralization analysis, chemical analysis of selected leachates and numerical simulation to identify the minerals controlling the leaching behavior of stabilized hydroxide sludge. This second part deals with the use of numerical simulation as an aid tool for the identification of the minerals. The framework for minerals identification is based on the study of minerals stability in function of the geochemical context using numerical simulation. A mineral assemblage permitting the simulation of a pH dependence leaching test (acid neutralization and release of elements) has been identified for the four studied cement pastes. Therefore, the proposed methodology is a pertinent tool for the modeling of the leaching behavior of inorganic wastes.

© 2009 Elsevier Ltd. All rights reserved.

1. Introduction

To control the risk for environment of the disposal of stabilized/solidified wastes, legislations impose to assess their leaching behavior. In the last decade, behavioral modeling became a useful tool in ecological risk assessment to estimate the release of pollutants in disposal conditions [1,2]. Due to the complexity of the reactions controlling the mobilizations of the pollutants, geochemical modeling is more and more used to represent the leaching behavior of inorganic wastes. Therefore, the development of a behavioral model to describe the leaching of stabilized/solidified wastes requires a minimal knowledge of their mineralogy [3].

Links between mineralogy and leaching behavior can be approached through saturation index calculations, that permits to identify the minerals possibly in equilibrium (or close to equilibrium) with the leachates coming from leaching tests [4–6]. However, saturation indexes can be calculated only for the phases containing the analyzed elements. Therefore, the resulting list of minerals close to equilibrium with leachates is not exhaustive. For example, carbonated phases are often forgotten by such calculations.

The differential analysis of acid neutralization data proposed by Glass and Buenfeld [7] permits a mineralogical interpretation of the

leaching behavior of cementitious pastes. However, the identification of hydrates remains fairly complex because of the influences of the geochemical context on the stability of cementitious phases [7–9].

Based on the thermodynamic equilibrium laws [3], geochemical models are designed to simulate chemical reactions in water systems in contact with solid and gas phases. These models are able to predict the theoretical response to an acid attack of minerals in various geochemical contexts. Therefore, geochemical modeling could be an interesting tool to study the stability of hydrated cement phase.

In this two parts paper, we propose to characterize and to model the leaching behavior of stabilized/solidified sludge doped in zinc and chromium. The part I [10] deals with the experiments (difference acid neutralization analysis, chemical analysis of selected leachates, SEM-EDS observations and XRD) implemented to establish the links between leaching and mineralogy. In this second part, we propose to use numerical simulation as an aid tool to interpret experimental results, in particular those of the differential acid neutralization analysis test. In this paper, our attention is focused on the implementation of a model (mineral assemblage) able to represent the behavior of the main hydrates because they are controlling the evolution of pH and, thus, the release of pollutants. Nevertheless, some hypotheses about the behavior of zinc and chromium were tested.

Numerous hypotheses can be formulated from experimental results to explain the leaching behavior. Nevertheless they can hardly be confirmed. In this work, a framework is proposed to use geochemical

* Corresponding author. Tel.: +33 4 72 43 88 41; fax: +33 4 72 43 87 17.

E-mail address: olivier.peyronnard@uqat.ca (O. Peyronnard).

calculations as an aid tool to identify and quantify the minerals controlling the leaching behavior of stabilized hydroxide sludge. Numerical simulation were performed using USGS's software PHREEQC [11], that has been successfully used to model the leaching behavior of cement stabilized/solidified wastes [12–14].

2. Experimental data [10]

Experiments were performed on synthetic hydroxide sludge, containing iron, zinc and hexavalent chromium. Sludge was stabilized/solidified by ordinary Portland cement (OPC, CEM I) or a mix of 50% of Portland cement and 50% of class F coal fly ashes (OPC-PFA). Four pastes were studied:

- two blanks containing only binders: OPC and OPC-PFA;
- two stabilized/solidified sludge: OPC-S and OPC-PFA-S.

Links between mineralogy and leaching behavior were investigated by differential acid neutralization analysis, chemical analysis of selected leachates, SEM-EDS observations and XRD. All the details on experimental conditions and the obtained results are presented in the part I of this paper [10].

3. Methodological framework for the identification of minerals

The identification of reactive minerals within cementitious composites using a numerical simulator is based on the assumption that numerical simulation permits to calculate the pH of dissolution of various hydrated phases in various environments. Thus, the comparison between simulated and experimental results should help for the identification of the cementitious hydrates. This comparison also

inform on the reaction path and the possible precipitations occurring during the acid attack.

A five step framework was followed to identify the mineral assemblages (mix of pure phases and solid solutions) representing the tested materials:

1. Estimation of the mineral phases potentially present or which could precipitate based on:
 - the knowledge of the studied material (bibliographic study, previous works...);
 - a mineralogical study by direct methods: XRD, SEM-EDS. Other methods like FTIR or thermal analysis can also be used;
 - the identification of phases potentially at equilibrium with the analyzed leachates by calculations of saturation index [4].
2. Simulation of the acid attack on simplified mineral assemblages issued from the previous step. These simulations permit the compilation of a bank of spectra adapted to the studied case. For cementitious materials like cement stabilized wastes, it is interesting to simulate the behaviors of cementitious composite considering the presence of portlandite and/or C-S-H.
3. Minerals identification and quantification:
 - identification of the cementitious hydrates by comparison of the simulated and experimental spectra;
 - quantification from the area below peaks, the leachable fraction or the total content of elements.
4. Simulation of the behavior of the mineral assemblage determined at the previous step and comparison with experimental results. This comparison is made on the differential analysis spectra, the titration curves and the release of elements. Step 3 and 4 are reiterated until the obtaining of an acceptable simulation.

Table 1
Reactions and equilibrium constants for minerals considered in the minerals assemblages representing the four studied materials.

Mineral	Reaction	Log K_1 [ref]	Log K_2 [ref]
Portlandite	$\text{Ca(OH)}_2 + 2\text{H}^+ \leftrightarrow \text{Ca}^{2+} + 2\text{H}_2\text{O}$	22.8 [15]	22.555 [16] 22.9 [20]
Brucite	$\text{Mg(OH)}_2 + 2\text{H}^+ \leftrightarrow \text{Mg}^{2+} + 2\text{H}_2\text{O}$	16.84 [15]	
Zn(OH) ₂	$\text{Zn(OH)}_2 + 2\text{H}^+ \leftrightarrow \text{Zn}^{2+} + 2\text{H}_2\text{O}$	11.9 [16]	
Ca-hydroxizincate	$\text{CaZn}_2(\text{OH})_6 : 2\text{H}_2\text{O} + 6\text{H}^+ \leftrightarrow \text{Ca}^{2+} + 2\text{Zn}^{2+} + 8\text{H}_2\text{O}$	43.9 [17]	
Gypsum	$\text{CaSO}_4 : 2\text{H}_2\text{O} \leftrightarrow \text{Ca}^{2+} + \text{SO}_4^{2-} + 2\text{H}_2\text{O}$	–4.581 [15]	–4.48 [16]
Al(OH) ₃ (am)	$\text{Al(OH)}_3 + \text{OH}^- \leftrightarrow \text{Al(OH)}_4^-$	0.24 [18]	
Fe(OH) ₃ (am)	$\text{Fe(OH)}_3 + 3\text{H}^+ \leftrightarrow \text{Fe}^{3+} + 3\text{H}_2\text{O}$	5 [15]	
SiO ₂ (am)	$\text{SiO}_2 + 2\text{H}_2\text{O} \leftrightarrow \text{Si(OH)}_4$	–2.714 [15–17]	
C ₂ ASH ₈	$\text{Ca}_2\text{Al}_2\text{O}_5\text{SiO}_2 : 8\text{H}_2\text{O} \leftrightarrow 2\text{Ca}^{2+} + 2\text{Al(OH)}_4^- + \text{Si(OH)}_3^- + \text{OH}^- + 2\text{H}_2\text{O}$	–20.49 [19]	
C-S-H			
C-S-H1.8	$(\text{CaO})_{1.8}\text{SiO}_2 : 1.8\text{H}_2\text{O} + 3.6\text{H}^+ \leftrightarrow 1.8\text{Ca}^{2+} + \text{Si(OH)}_4 + 1.6\text{H}_2\text{O}$	32.6 [13]	
	$\text{Ca}_{1.8}\text{SiO}_{3.8} : \text{H}_2\text{O} + 3.6\text{H}^+ \leftrightarrow 1.8\text{Ca}^{2+} + \text{Si(OH)}_4 + 0.8\text{H}_2\text{O}$		32.7 [20]
C-S-H1.1	$(\text{CaO})_{1.1}\text{SiO}_2 : 1.1\text{H}_2\text{O} + 2.2\text{H}^+ \leftrightarrow 1.1\text{Ca}^{2+} + \text{Si(OH)}_4 + 0.2\text{H}_2\text{O}$	16.7 [13]	
	$\text{Ca}_{1.1}\text{SiO}_{3.1} : \text{H}_2\text{O} + 2.2\text{H}^+ \leftrightarrow 1.1\text{Ca}^{2+} + \text{Si(OH)}_4 + 0.1\text{H}_2\text{O}$		16.72 [20]
C-S-H0.8	$(\text{CaO})_{0.8}\text{SiO}_2 : 0.8\text{H}_2\text{O} + 1.6\text{H}^+ + 0.4\text{H}_2\text{O} \leftrightarrow 0.8\text{Ca}^{2+} + \text{Si(OH)}_4$	11.1 [13]	
	$\text{Ca}_{0.8}\text{SiO}_{2.8} : \text{H}_2\text{O} + 1.6\text{H}^+ + 0.2\text{H}_2\text{O} \leftrightarrow 0.8\text{Ca}^{2+} + \text{Si(OH)}_4$		11.08 [20]
Afm			
Al-monosulfate	$(\text{CaO})_3\text{Al}_2\text{O}_3\text{CaSO}_4 : 12\text{H}_2\text{O} \leftrightarrow 4\text{Ca}^{2+} + 2\text{Al(OH)}_4^- + \text{SO}_4^{2-} + 4\text{OH}^- + 6\text{H}_2\text{O}$	–29.43 [21]	–27.62 [22]
Fe-monosulfate	$(\text{CaO})_3\text{Fe}_2\text{O}_3\text{CaSO}_4 : 12\text{H}_2\text{O} \leftrightarrow 4\text{Ca}^{2+} + 2\text{Fe(OH)}_4^- + \text{SO}_4^{2-} + 4\text{OH}^- + 6\text{H}_2\text{O}$	–32.02 [19]	
Cr-monophase	$(\text{CaO})_3\text{Al}_2\text{O}_3\text{CaCrO}_4 : 15\text{H}_2\text{O} \leftrightarrow 4\text{Ca}^{2+} + 2\text{Al(OH)}_4^- + \text{CrO}_4^{2-} + 4\text{OH}^- + 9\text{H}_2\text{O}$	–30.38 [23]	
Al-monocarbonate	$(\text{CaO})_3\text{Al}_2\text{O}_3\text{CaCO}_3 : 11\text{H}_2\text{O} \leftrightarrow 4\text{Ca}^{2+} + 2\text{Al(OH)}_4^- + \text{CO}_3^{2-} + 4\text{OH}^- + 5\text{H}_2\text{O}$	–31.47 [19]	
Fe-monocarbonate	$(\text{CaO})_3\text{Fe}_2\text{O}_3\text{CaCO}_3 : 11\text{H}_2\text{O} \leftrightarrow 4\text{Ca}^{2+} + 2\text{Fe(OH)}_4^- + \text{CO}_3^{2-} + 4\text{OH}^- + 5\text{H}_2\text{O}$	–35.79 [19]	
Friedel's salt	$(\text{CaO})_3\text{Al}_2\text{O}_3\text{CaCl}_2 : 10\text{H}_2\text{O} \leftrightarrow 4\text{Ca}^{2+} + 2\text{Al(OH)}_4^- + 2\text{Cl}^- + 4\text{OH}^- + 4\text{H}_2\text{O}$	–28.8 [14]	
C ₄ AH ₁₃	$(\text{CaO})_4\text{Al}_2\text{O}_3 : 13\text{H}_2\text{O} \leftrightarrow 4\text{Ca}^{2+} + 2\text{Al(OH)}_4^- + 6\text{OH}^- + 6\text{H}_2\text{O}$	–27.49 [22]	
	$(\text{CaO})_4\text{Al}_2\text{O}_3 : 13\text{H}_2\text{O} + 14\text{H}^+ \leftrightarrow 4\text{Ca}^{2+} + 2\text{Al}^{3+} + 20\text{H}_2\text{O}$		107.25 [16]
C ₄ FH ₁₃	$(\text{CaO})_4\text{Fe}_2\text{O}_3 : 13\text{H}_2\text{O} \leftrightarrow 4\text{Ca}^{2+} + 2\text{Fe(OH)}_4^- + 6\text{OH}^- + 6\text{H}_2\text{O}$	–29.88 [19]	
Aft			
Ettringite	$\text{Ca}_6\text{Al}_2(\text{SO}_4)_3(\text{OH})_{12} : 26\text{H}_2\text{O} \leftrightarrow 6\text{Ca}^{2+} + 2\text{Al(OH)}_4^- + 3\text{SO}_4^{2-} + 4\text{OH}^- + 26\text{H}_2\text{O}$	–45.09 [19]	
	$\text{Ca}_6\text{Al}_2(\text{SO}_4)_3(\text{OH})_{12} : 26\text{H}_2\text{O} + 12\text{H}^+ \leftrightarrow 6\text{Ca}^{2+} + 2\text{Al}^{3+} + 3\text{SO}_4^{2-} + 38\text{H}_2\text{O}$		62.536 [16]
Fe-ettringite	$\text{Ca}_6\text{Fe}_2(\text{SO}_4)_3(\text{OH})_{12} : 26\text{H}_2\text{O} \leftrightarrow 6\text{Ca}^{2+} + 2\text{Fe(OH)}_4^- + 3\text{SO}_4^{2-} + 4\text{OH}^- + 26\text{H}_2\text{O}$	–49.49 [19]	
Cr-ettringite	$\text{Ca}_6\text{Al}_2(\text{CrO}_4)_3(\text{OH})_{12} : 26\text{H}_2\text{O} \leftrightarrow 6\text{Ca}^{2+} + 2\text{Al(OH)}_4^- + 3\text{CrO}_4^{2-} + 4\text{OH}^- + 26\text{H}_2\text{O}$	–41.46 [23]	
Al-tricarbonate	$\text{Ca}_6\text{Al}_2(\text{CO}_3)_3(\text{OH})_{12} : 26\text{H}_2\text{O} \leftrightarrow 6\text{Ca}^{2+} + 2\text{Al(OH)}_4^- + 3\text{CO}_3^{2-} + 4\text{OH}^- + 26\text{H}_2\text{O}$	–41.3 [19]	

Log K_1 correspond to the solubility product used during minerals identification; log K_2 was used to study the influence of thermodynamic data on simulation results. Values are given for a temperature of 25 °C.

Table 2
Mineral assemblages representing the four studied materials.

Phases	OPC	OPC-PFA	OPC-S	OPC-PFA-S
Portlandite	2,2 (EP)	0,80 (EP)	0,4 (EP)	0,08 (EP)
Brucite	0,08 (EP)	0,14 (EP)	0,06 (EP)	0,12 (EP)
Zn(OH) ₂	3,2.10 ⁻⁴ (EP)	0 ^a (EP)	0 ^a (EP)	0 ^a (EP)
Ca-hydroxizincate		4.10 ⁻⁵ (EP)	0,03 (EP)	0,03 (EP)
C ₂ ASH ₈	0 ^a (EP)	0 ^a (EP)	0 ^a (EP)	0,18 (EP)
Fe(OH) ₃	0 ^a (EP)	0 ^a (EP)	0 ^a (EP)	0 ^a (EP)
Al(OH) ₃	0 ^a (EP)	0 ^a (EP)	0 ^a (EP)	0 ^a (EP)
SiO ₂ (am)	0 ^a (EP)	0 ^a (EP)	0 ^a (EP)	0 ^a (EP)
Gypsum	0 ^a (EP)	0 ^a (EP)	0 ^a (EP)	0 ^a (EP)
C-S-H1.8	2 (SS)	0,2 (SS)	0,8 (SS)	0,24 (SS)
C-S-H1.1	1 (SS)	2 (SS)	0,8 (SS)	1,2 (SS)
C-S-H0.8	0 ^a (SS)	0 ^a (SS)	0 ^a (SS)	0 ^a (SS)
Al-monosulfate	0,12 (SS)	0,16 (SS)		
Fe-monosulfate	0,04 (SS)	0,16 (SS)	0,28 (SS)	0,1 (SS)
Cr-monophase	3,6.10 ⁻⁵ (SS)	1,2.10 ⁻⁴ (SS)	0 ^a (SS)	0 ^a (SS)
Al-monocarbonate	0,72 (SS)	0,24 (SS)	0,32 (SS)	0,04 (SS)
Fe-monocarbonate	0,32 (SS)	0,12 (EP-DO)	0,4 (EP-DO)	0,08 (EP)
Friedel's salt			0,06 (SS)	
Ettringite	0,16 (SS)	0,04 (SS)	0,04 (SS)	0,02 (SS)
Fe-ettringite	0,08 (SS)			
Cr-ettringite	0 ^a (SS)	0 ^a (SS)	8.10 ⁻⁵ (SS)	0 ^a (SS)
Al-tricarbonate	0 ^a (SS)	0,04 (SS)	0,04 (SS)	0,16 (SS)
C ₄ AH ₁₃			0,24 (SS)	
C ₄ FH ₁₃			0,24 (SS)	

SS: solid solution; EP: equilibrium phases; DO: dissolve only. Phases' amounts are expressed in mmol/g of solid.

^a Phases precipitating during the leaching process.

5. Validation of the identified mineral assemblage by comparison of the simulated and experimental results of a leaching test conducted under different conditions. In our case, the validation was made on a pH dependence test realized at a liquid/solid ratio of 10.

4. Hypotheses of simulation

Acid attacks were simulated using the USGS's software PHREEQC [11]. PHREEQC is a geochemical calculations software based on the laws of equilibrium between solid, liquid and gas phases. The following hypotheses were considered for the simulations:

- The equilibrium between liquid and solid is reached, no gas phase is considered.
- Cementitious phases are considered as pure phases (EQUILIBRIUM_PHASES) or as forming ideal solid solutions (SOLID_SOLUTIONS). No sorption mechanisms are considered. Phases, which could precipitate during the leaching, are integrated in the mineral assemblage with an initial amount equal to 0.
- Amorphous C-S-H is integrated in the thermodynamic database considering 3 calcium silicate hydrates having Ca/Si ratios equal to 1.8, 1.1 and 0.8 to model their non congruent dissolution [13]. In the mineral assemblage, they are considered as forming a solid solution in order to smooth the transition from the C-S-H rich in calcium to the C-S-H poor in calcium.

As in most of geochemical calculation software, thermodynamic data are, in PHREEQC regrouped in a thermodynamic database. To be pertinent, the proposed methodology needs a database as exhaustive as possible. So, a database dedicated to hydrated cement materials containing zinc and chromium was compiled. Clinker phases (C₂S, C₃S, C₃A and C₄AF) were not included in the database because no log K values of their dissolution were found in the literature. Moreover, calculations were made considering the reaching of the equilibrium between solid and liquid phases. Therefore, due to the large amount of water, even if clinker phases were added in the mineral assemblages, calculations would result in their immediate dissolution and reprecipitation as hydrated phases.

The Table 1 presents the solubility products and the dissolution reactions of the phases used to represent the leaching behavior of our materials. The database compilation shows divergences on solubility products between authors, even for well known phases like portlandite. We choose to use the values (log K₁) the more quoted in the literature. To test the robustness of our methodology, the influence of thermodynamic data on simulation results was analyzed using, for some phases, other values found in the literature (log K₂).

5. Simulation results

5.1. Identification and quantification of mineral phases

The Table 2 presents the mineral assemblages used to represent the behavior of the four studied pastes when submitted to an acid neutralization test. For each paste, phases are set, in the mineral assemblage, at their identified amount in the solid. Phases, set at an amount equal to zero, are not present in the unleached material, but precipitate during the leaching process. The release of sodium and potassium being independent of pH variations [10], they are integrated as solute in the leaching solution.

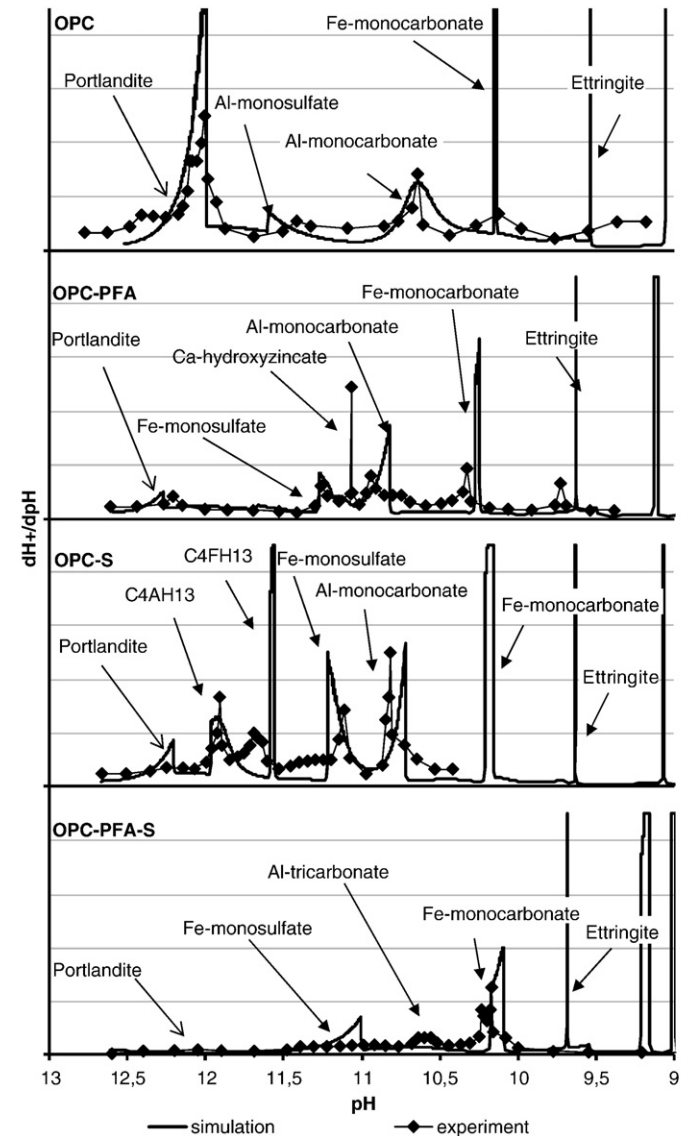


Fig. 1. Identification of the mineral assemblages: experimental and simulated spectra (a. OPC, b. OPC-PFA, c. OPC-S and d. OPC-PFA-S).

In Table 2, it is shown that the four studied pastes are mainly composed of the same hydrates: portlandite, C-S-H, AFm and AFt phases. The influence of fly ash and hydroxide sludge on cement hydration consists principally in variations of phases' amounts. As it can be expected, portlandite is highly consumed by pozzolanic reactions in OPC-PFA and OPC-PFA-S. For OPC-S and OPC-PFA-S, a relative increase in AFm and AFt amounts can, also, be remarked. It can be explained by the inhibition of C₂S and C₃S hydration caused by zinc: C₂S and C₃S being less hydrated, C₃A and C₄AF's hydration products are precipitated with relatively higher amounts. The localization of sulfates also differs for the material containing sludge (OPC-S and OPC-PFA-S). Due to the sludge's sulfate content (4.4% in mass), sulfate is mainly precipitated as ettringite in these two pastes whereas it forms Al-monosulfate in OPC and OPC-PFA. It is explained by the C₃A's hydration reaction path. In Portland cement, C₃A is, first, hydrated as ettringite that is step by step transformed in Al-monosulfate with the drop of sulfates concentration [24]. For OPC-S and OPC-PFA-S, the sulfates amounts being higher, this transformation of AFt into AFm is limited. The use of PFA as binder also induces a silicon enrichment of C-S-H: C-S-H is mainly modeled by calcium silicate hydrates having Ca/Si ratio equal to 1.1 whereas C-S-H are enriched in C-S-H1.8 in OPC and OPC-S. Finally, in OPC-S, the sludge load induces the precipitation of hydrates not observed in the other pastes: C₄AH₁₃ and C₄FH₁₃.

It is to be noted that the mineral assemblages presented in Table 2 are not representative of pastes' mineralogy but of their fraction that is reactive to the leaching. In other words, some phases present in the pastes can be not identified because of their weak influence on the leaching behavior. For example, quartz is present in PFA and also in OPC-PFA and OPC-PFA-S but it can be neglected in their mineral assemblage because of its very low solubility. Nevertheless, as it can be seen for chromates, the proposed method can be enough sensitive to identify the phases controlling the behavior of trace elements.

The Fig. 1 represents, for the four studied pastes, the experimental and simulated spectra. It can be seen in this figure that the pH evolution of leachate is, mainly, controlled by the dissolution of three groups of hydrates:

- In the first time, the pH remains high (up to 12) because of the dissolution of portlandite. For OPC-S, the dissolution of C₄AH₁₃ and C₄FH₁₃ buffers the leachates at pH respectively equal to 11.9 and 11.7.
- For pH between 11.5 and 10, the leaching is mainly controlled by the dissolution of AFm phases: aluminum and iron monosulfates for pH up to 11 and aluminum and iron monocarbonate for pH between 11 and 10. AFm phases are known to form solid solutions [24,25], therefore they have generally been introduced as such in the mineral assemblages (Table 2).
- The decrease of pH under 10 is then controlled by the dissolution of AFt, C₂ASH₈ and C-S-H. However, due to a lack of experimental data, the phases have mainly been identified from the release of sulfates and silicon. Therefore, identification and quantification of minerals remain imprecise. Like AFm, AFt phases have been considered as forming a solid solution.

The Fig. 2 represents the evolution of the mineral assemblages among the decrease of pH. It shows that some phases precipitate from the elements released. Indeed, the dissolution of AFm (e.g. monosulfates) is immediately followed by a reprecipitation of the released elements as AFt (e.g. ettringite). Due to the alkaline conditions, aluminum, iron and zinc can reprecipitate as hydroxides. Gypsum precipitates from the sulfates liberated by the dissolution of ettringite. Finally, the dissolution of C-S-H induces a precipitation of C₂ASH₈ and amorphous silica.

As stated previously, the identification and quantification of the reactive phases is made by comparison of differential analysis spectra, titration curves and the release of elements. Fig. 3 presents, as example, the curves of release of elements for OPC-PFA-S. This paste was chosen because the conclusions about the ability of the models to

represent elements' release are representative of the observations made for the other pastes:

- the release of calcium is well represented;
- the simulations give a too weak silicon release for pH over 11 and a too high release for pH under 11. It is probably due to the simplified

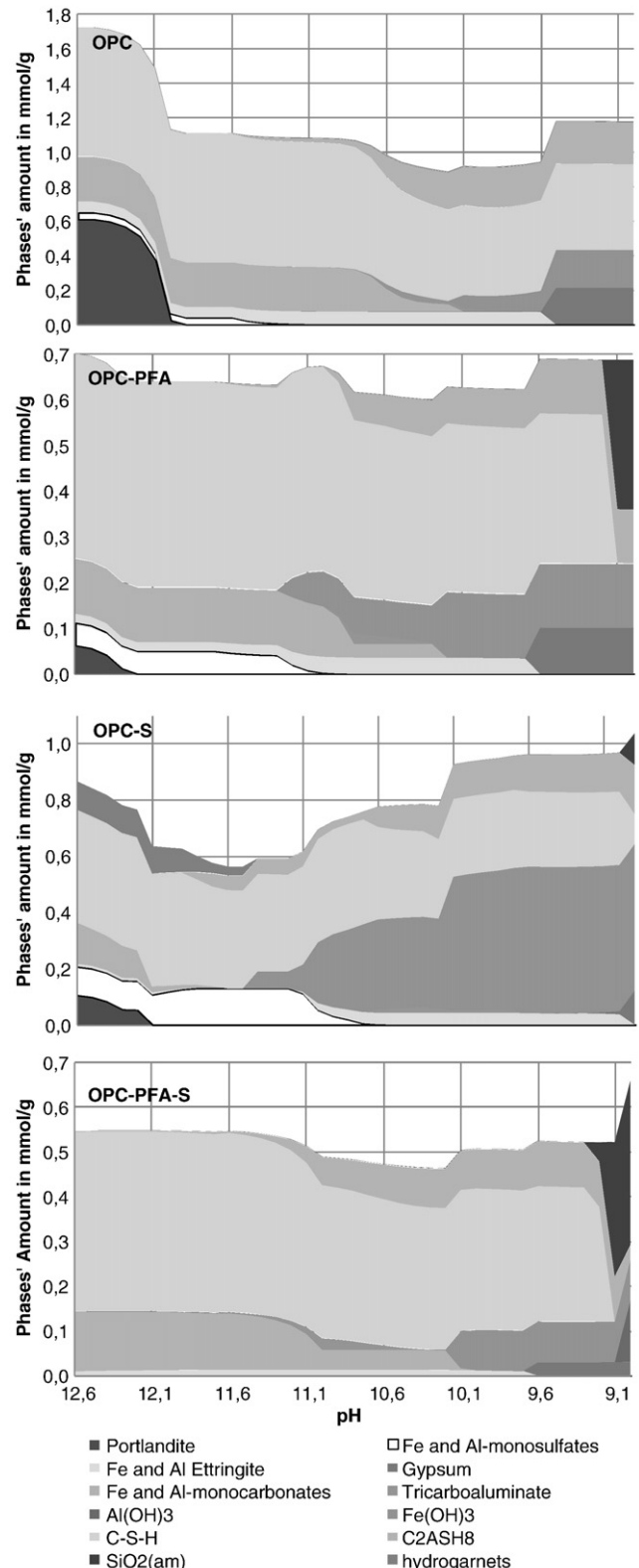


Fig. 2. Evolutions of the mineral assemblages among the decrease of pH.

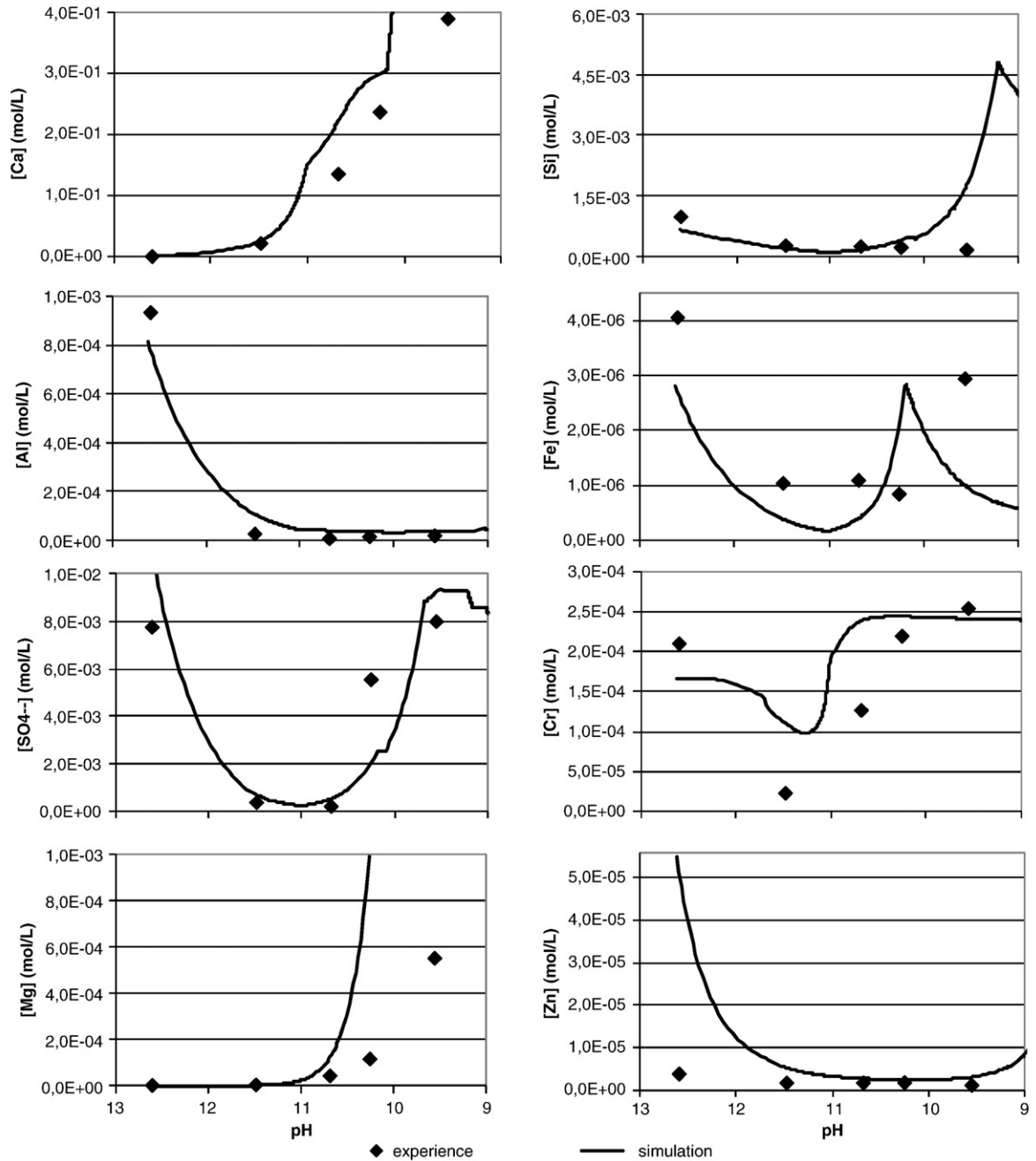


Fig. 3. Experimental and simulated leaching curves of OPC-PFA-S.

model chosen to represent the dissolution of C-S-H. It is able to represent correctly the decalcification but no silicon is released until the dissolution of C-S-H's siliceous structure. The too high release for the lower pH can be explained by an inaccurate value of the log K used to represent the solubility of amorphous silica.

- Aluminum and iron are present in various cementitious hydrates (AFm, AFt...) and possibly reprecipitate under new forms (AFt, amorphous hydroxides). This induces variations of release that are hardly represented with a simplified mineral assemblage. Nevertheless, the identified mineral assemblages permit to simulate correctly the most important evolutions of leaching.
- The control by ettringite dissolution of the release of sulfate is clearly demonstrated for the four materials. For OPC and OPC-PFA, ettringite is too soluble in highly basic conditions to represent correctly the observed mobilization but considering sulfate as AFm gives good results. In highly basic conditions, the

release of sulfates is controlled by monosulfate, then, ettringite precipitates from the sulfate and aluminum liberated and controls the leaching. For lower pH (<9.6), the release of sulfates is controlled by gypsum that precipitates after the dissolution of ettringite.

- The observed link between chromium and sulfate release is well represented by considering sulfates substitution by chromates in AFm and AFt phases. To permit a good representation of chromium release, it is important to model AFm and AFt as solid solutions.
- The released of zinc is globally well represented by considering it as forming calcium hydroxizincate or hydroxide. Nevertheless, for the higher pH (>12), simulations calculate a too high release. It can be due to the choice made to represent zinc. Indeed, we choose to model it as precipitated but, others mechanisms, not tested here, could explain zinc retention. For example, adsorption on the surface of C-S-H is frequently cited in literature [26].

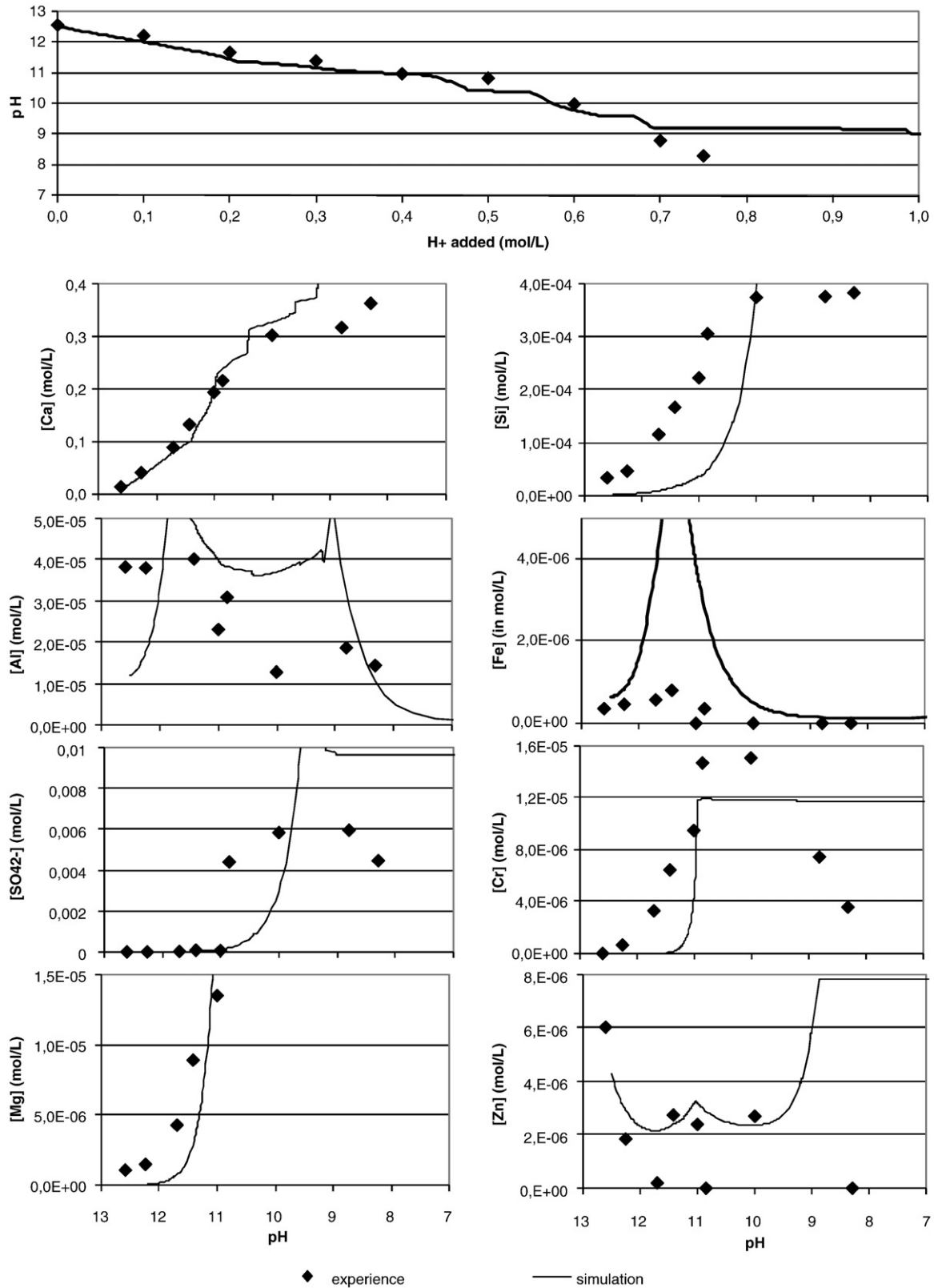


Fig. 4. Experimental and simulated results of the validation of the mineral assemblage representing OPC-PFA.

5.2. Mineral assemblages' validation

To be valid, a model has to be able to simulate the behavior in conditions differing from those used for its elaboration. One of the ways to validate a model is to check its ability to simulate an experiment

conducted in conditions differing from those used for its implementation [1]. The validation of our mineral assemblages was made using the results of a pH influence test conducted at Liquid/Solid ratio equal to 10 (against 4 for the test used for the identification) for pH between natural pH (pH obtained at the equilibrium between the material and pure water) and 7.

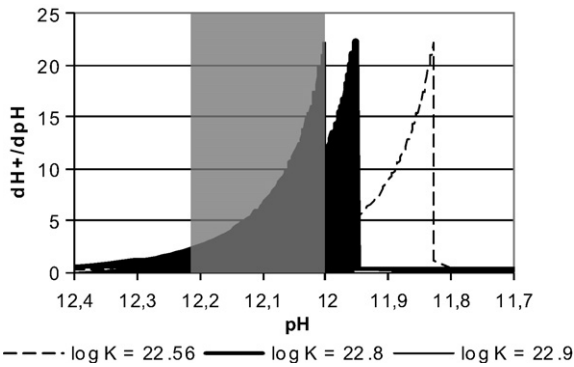


Fig. 5. Influence of the solubility product on the dissolution of portlandite.

Fig. 3 presents, as example, the validation results for OPC-PFA. The conclusions drawn from the three other materials are similar. Simulations results show a good ability of the identified mineral assemblages to simulate the leaching behaviors while pH remains above 10. For lower pH, important divergences between experimental and predicted results are observed in terms of buffering capacities and releases of elements. It comes from an incorrect identification and quantification of the hydrated phases controlling the leaching behavior in “acid” conditions. For example, experimental results show, for OPC-PFA, a decrease of sulfates’ release when the pH decreases below 9 whereas simulation calculates a constant release. Therefore, the control of sulfate release by gypsum is not adapted to describe the sulfates’ behavior after the dissolution of ettringite. The buffering at a pH around 9.1, observed on the simulation results of OPC-PFA but not on experimental results, shows the inability of the C-S-H model to represent correctly their dissolution, in particular the dissolution of their siliceous structure. This incorrect identification of the phases controlling the leaching behavior for pH lower than 10 is due to a lack of experimental data. Indeed, experiments were performed for pH down to 9.5, thus data miss to elaborate a reliable model for pH under 10.

For some elements, simulated results don’t fit to experiments all along the investigated range of pH. The release of silicon is too weak for pH higher than 10 where silicon becomes too highly leached. As stated previously, it is due to the model chosen to represent C-S-H incongruent dissolution. The release of sulfates and chromium, are also badly simulated with an increase of experimental leaching for a pH higher than the simulated one. A similar shift of sulfates and chromium’s release is observed when comparing the experimental results obtained with the two L/S ratios (L/S = 4, Fig. 4 and L/S = 10, Fig. 5). For L/S equal 4, the release of sulfates is explained by the precipitation of ettringite simultaneously of monosulfates dissolution. For higher L/S, experimental results tend to show that ettringite

doesn’t precipitate, probably because of a dilution effect, whereas calculations result in a precipitation of ettringite for L/S equal 10. This simulation error can be due to the values of log K used to represent the dissolution of ettringite. For iron and aluminum, simulations show a behavior more complex than the observed one with variations of the release not shown by the experimental leaching curves. For L/S equal 4, the identified mineral assemblages explain the release of Al and Fe by the dissolution of AFm followed by a reprecipitation as AFt. For L/S equal 10, due to a dilution effect, calculations lightly “retard” the reprecipitation of Al and Fe. Like for sulfates, this simulation error can be attributed to the log K used to represent AFt and AFm dissolution.

To conclude, the comparison between experimental and simulation results for the experiment conducted at a L/S ratio of 10 doesn’t permit a total validation of the identified mineral assemblages. Nevertheless, as it can be seen, the mineral assemblages permit a good simulation of the experiment while the pH remains higher than 10. Therefore to be pertinent, the mineral assemblages required to be identified from experimental results including the whole range of pH that the solid could be confronted in real conditions. In other words, developing a leaching model based on geochemical calculations need to know the mineralogy of the unleached material but also its evolution during the leaching process. For sulfates, aluminum or iron, simulations error can, partially, be attributed to their values of dissolution log K. Therefore, to be suitable further works must be made to compile reliable thermodynamics databases.

6. Discussions

6.1. Remarks on the experimental protocol

As seen in the last paragraph, the range of pH investigated during the differential acid neutralization analysis test should be extended to lower pH in order to facilitate the identification and quantification of the phases controlling the leaching behavior for pH below 10. As seen in the precedent sections, the dissolution of the mains cementitious hydrates occurs for pH higher than 10 but C-S-H or AFt phases remain present for pH around 9. Therefore, the investigated range of pH should be extended until pH around 8. This larger range also permits a better estimation of the leachable fraction of the elements having a release increasing with the decrease of pH.

The analysis of the chemical composition of the two solutions before and after each peak of the differential analysis spectra would also refine the understanding of the leaching behavior of the studied materials. Indeed, that permits to clearly identify the elements released by the dissolutions inducing the peaks and the elements leached independently of the dissolutions of the main phases. Moreover, it permits to refine the nature of phases identified as close to equilibrium with the leachates by saturation index calculations.

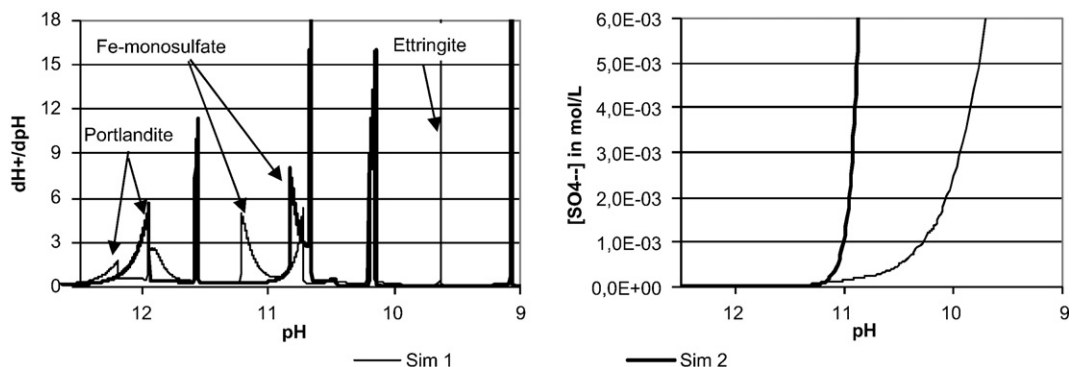


Fig. 6. Influence of the solubility products on the leaching behavior of the mineral assemblage representing OPC-S.

6.2. Remarks on the identification of a representative mineral assemblage

To give suitable results, the minerals assemblages must be calibrated by the comparison of simulated and experimental differential analysis spectra, simulated and experimental titration curves and simulated and experimental leaching curves. Indeed, a mineral assemblage permitting a reasonably good differential analysis spectrum can be unable to simulate correctly the release of elements. Moreover, because of the difference of leaching behavior induced by variations of the mineral amounts, the hydrates quantification has to be made simultaneously of their identification. For example, Fe-monocarbonate appears in both OPC-PFA and OPC-PFA-S, but its dissolution is observed at pH around 10.3 for OPC-PFA and around 10.2 for OPC-PFA-S. This shift is due to aluminum tricarbonatite dissolution: present in larger quantity in OPC-PFA-S, its dissolution delays Fe-monosulfate's one. This quantification of hydrates can be, in a first time, obtained from the acid consumption required for their dissolution (area below peaks). It is, then, refined by fitting simulation results on titration curve and elements release.

Determining a mineral assemblage to represent the leaching behavior of material required to make compromises to represent correctly the release of elements, the differential analysis spectrum and the titration curve. For example, a better representation of the calcium release could be obtained by reducing the amount of AFm phases, but, then, the acid neutralization capacity became too weak. We can, also, remark that the proportions of C-S-H1.8 and C-S-H1.1 play an important role in the amount of calcium released and in the shape of the titration curve from the start of the acidification.

6.3. Capacities and limits of the methodology

In this two parts paper, a methodology coupling differential acid neutralization analysis, chemical analysis of selected leachates and utilization of geochemical to identify reactive minerals was used to characterize the leaching behavior of hydroxide sludge stabilized by hydraulic binders. This methodology appears as an interesting tool to link the mineralogy and the leaching of cementitious materials:

- the differential analysis highlights the role of each hydrated phase on the resistance to acidification;
- the chemical analysis of selected leachates permits to describe the evolution of elements' release. It also permits to highlight the possible links between the release of pollutants and the dissolution of main hydrates: chromium release appears linked to AFm or AFt dissolution and a phase containing zinc is dissolved for a pH around 11;
- the using of numerical simulation to test the hypotheses made to explain the experimental results and, thus, facilitate their interpretation. Moreover, the framework, proposed to identify the dissolving minerals (§ III), has permit, for each paste, the elaboration of a model (mineral assemblage) representing their fraction reactive to the leaching process.

The identification of a mineral assemblage for each studied cement paste shows the success of our methodology to develop a leaching model of such materials. Nevertheless, due to the experimental conditions (reactions in batch until attainment of equilibrium, high L/S ratio...) some precautions have to be taken when using these mineral assemblages to extrapolate experimental results to realistic conditions of exposition. Indeed, the identified mineral assemblages integrate phases initially present in the unleached material and phases precipitating during the leaching. Nevertheless, the phases that will precipitate in realistic condition could be different from those identified because of differences of the geochemical context: release of elements caused by transport mechanisms, lower L/S. Therefore, the proposed methodology permits to identify the dissolving minerals initially present, and

informs on possible precipitating phases, other precipitation reactions could occur depending on the geochemical context.

The proposed methodology was successful to develop a leaching model for cement paste and we think that it can be successfully used for other kinds of inorganic wastes or more complex cementitious matrixes. Nevertheless, in this study, the mineral assemblages could be identified because of the relative knowledge of cementitious pastes behavior. For new materials, the methodology will give good results if it's coupled with other mineralogical analysis by "classical" techniques (XRD, SEM-EDS, thermal analysis, spectrometry...). In order to investigate the mineralogical evolution during the leaching process, these analysis could be performed on leached materials. Like for chemical analysis of leachates, it would be very pertinent to base the selection of leached materials on differential analysis spectra.

6.4. Robustness of the methodology

When compiling the thermodynamic data, different values of the dissolution reactions solubility products were found in the literature. In order to test the robustness of the mineral identification framework described in this paper, the influence of solubility products' values on simulation results was analyzed. This study was focalized on the behavior of a pure phase (portlandite) and on the mineral assemblage representing OPC-S. For portlandite, three simulations were made with $\log K$ equal to 22.8, 22.555 and 22.9. For OPC-S's mineral assemblage, two simulations were made: the first one (Sim 1) using the $\log K_1$ of the Table 1, the second (Sim 2) the $\log K_2$.

For a pure phase, the influence of the solubility product value can't be neglected. For portlandite (Fig. 5) the shift, reaching 0.2 pH unit, is over the uncertainty on pH measurement (0.1 pH unit). However, the presence of two phases, dissolving in a range of pH lower than 0.2, would result in unique peak on differential analysis spectrum because of the uncertainty of pH measurement. Therefore, the influence of $\log K$ values on simulation results would not induce additional identification error to those due to the superposition of peaks.

On the contrary, the influence of solubility products on the behavior of an assemblage of several minerals could induce some misinterpretations of differential analysis spectra. Indeed, Fig. 6 shows important changes of simulations results: important gaps shifts in the dissolution pH of phases and changes of the reaction path. For example, Fe-monosulfate is dissolving at pH around 11.2 in Sim 1 against 10.8 in Sim 2. Moreover, in Sim 1, some ettringite is precipitating from the sulfate liberated by the Fe-monosulfate dissolution and the aluminum coming from C_3AH_{13} and Al-monocarbonate. Then, ettringite dissolves for pH around 9.7 explaining the observed release of sulfate. In Sim 2, no ettringite precipitates, therefore, sulfates are leached at pH around 10.8 (Fig. 6).

Therefore, simulations results depending of the used solubility products, the thermodynamic database have an influence on the mineral assemblage identified to represent a material. The proposed method can't be considered as robust. However, these results more question the reliability of the used thermodynamic data than the validity of the presented framework. Actually, the validation of mineral assemblages shows their ability to simulate the behavior of the material in other conditions. Moreover, our methodology is based on the fitting of parameters (nature and amount of phases) on two different kinds of outputs: acid neutralization data (titration curve and differential analysis spectra) and release of elements.

7. Conclusions

This study deals with the characterization and the modeling of the leaching behavior of synthetic hydroxide sludge stabilized/solidified by hydraulic binders. The methodology developed in this work couple a differential analysis of acid neutralization data, a chemical analysis of leachates selected on differential analysis spectrum and the identification

of the dissolving minerals using numerical simulation. In this second part, the possibility of using numerical simulation as an aid tool to interpret the experimental results is investigated. A framework, based on the study of hydrated cement phases' stability in various geochemical contexts, is proposed for the identification of the reactive minerals.

The proposed methodology proves to be an efficient tool for the modeling of the leaching behavior of cementitious matrixes:

- the differential analysis of acid neutralization data highlights each dissolution reaction that occurs during the acidification;
- the chemical analysis of selected leachates permits to links the release of elements with this dissolution reactions. The release of main elements (Ca, Si, Al, SO_4^{2-} ...) informs on the nature of the dissolving minerals and the pollutants behavior informs on their retention/release mechanism.
- The using of numerical simulation for the identification of the minerals permits to test the validity of the hypotheses formulated to explain experimental results. It, also results in the identification of a mineral assemblage permitting the simulation of the leaching behavior of the studied matrixes.

The identified assemblages obtained show that the four studied pastes are mainly composed of the same hydrates (Portlandite, C-S-H and Aft/AFm phases) but at different amounts. The amount of portlandite decreases with the adding of fly ash or sludge due to pozzolanic reactions (PFA) and hydration inhibition (sludge). Sulfate forms ettringite in OPC-S and OPC-PFA-S whereas it forms monosulfates in OPC and OPC-PFA because of the sulfates contained in sludge. Finally, C-S-H are enriched in silicon for the fly ash cement (OPC-PFA and OPC-PFA-S).

The leaching behavior is controlled by the dissolution of hydrates: portlandite (pH ~ 12), monosulfates (pH between 11.5 and 11), monocarbonates (pH between 11 and 10.5), ettringite and other Aft (pH between 10.5 and 9.5) and, finally, dissolution of the siliceous structure of C-S-H (pH around 9.5–9). The leaching behavior is also controlled by some precipitation: aluminum and iron hydroxide, amorphous silica and Aft from the element released by the dissolution of AFm.

The proposed methodology appears as a useful tool for the modeling of the leaching behavior of cementitious matrixes. Nevertheless, the utilization of the mineral assemblages to extrapolate the experimental results to realistic conditions requires some precautions. Because of the difference of exposition conditions (transport of dissolved elements, kinetics of reaction, L/S...), it is possible that other precipitation reactions occur. Furthermore, the application of our methodology to other kinds of mineral materials requires a coupling with a fine mineralogical study of the materials before and during the leaching. Finally, it is shown that the reliability of the methodology and the simulations results highly depends on the reliability of the thermodynamic database. Therefore, further works are required to compile exhaustive (the most as possible) and reliable thermodynamic databases.

References

- [1] AFNOR NF EN 12920, Caractérisation des déchets - Méthodologie pour la détermination du comportement à la lixiviation d'un déchet dans des conditions spécifiées, AFNOR, 2006.

- [2] ADEME, Evaluation de l'écocompatibilité de scénarios de stockage et de valorisation des déchets, ADEME Editions, collection: Connaître pour Agir, 2002, 148 pp.
- [3] C. Zhu, G. Anderson, Environmental Applications of Geochemical Modeling, Cambridge University Press, Cambridge, 2002.
- [4] H.A. van der Sloot, A. van Zomeren, J.J. Dijkstra, J.C.L. Meussen, R.N.J. Comans, H. Scharf, Prediction of the Leaching Behaviour of Waste Mixture by Chemical Speciation Modelling Based on a Limited Set of Key Parameters, 2005 ECN RX 05-164 ECN (<http://www.ecn.nl/publications/default.aspx?nr=ECN-RX-05-164> consulted on 2009.0416).
- [5] G. Bröns-Laot, Evaluation environnementale de la valorisation de mâchefers d'incinération d'ordures ménagères en remplissage de carrière. Ph-D Thesis, INSA de Lyon, 2002.
- [6] Z. Rakotoarisoa, Prédiction du comportement environnemental des résidus de procédés thermiques (RPT) utilisés comme matériaux de travaux publics. Ph-D Thesis, INSA de Lyon, 2003.
- [7] G.K. Glass, N.R. Buenfeld, Differential acid neutralisation analysis, Cement and Concrete Research 29 (1999) 1681–1684.
- [8] J.A. Stegemann, R.J. Caldwell, C. Shi, Response of various solidification systems to acid addition, in: J.J.J. Goumans, G.J. Senden, H.A. van der Sloot (Eds.), Waste Materials in Construction: Putting Theory into Practice, Studies in Environmental Science, vol. 71, Elsevier Science, Amsterdam, 1997, pp. 803–814.
- [9] J.A. Stegemann, C. Shi, Waste acid resistance of different monolithic binders and solidified wastes, in: J.J.J. Goumans, G.J. Senden, H.A. van der Sloot (Eds.), Waste Materials in Construction: Putting Theory into Practice, Studies in Environmental Science, vol. 71, Elsevier Science, Amsterdam, 1997, pp. 551–562.
- [10] O. Peyronnard, M. Benzaazoua, D. Blanc, P. Moszkowicz, Study of Mineralogy and Leaching Behavior of Stabilized/Solidified Sludge Using Differential Acid Neutralization Analysis. Part I: Experimental Study, Cement and Concrete Research (2009) accepted ref CEMCON_3896.
- [11] D.L. Parkhurst, C.A.J. Appelo, User's Guide to Phreeqc (version 2) – A Computer Program for Speciation, Batch-Reaction, One-Dimensional Transport, and Inverse Geochemical Calculations, Water-Resources Investigations Report 99-4259, Denver, Colorado, 1999.
- [12] C.E. Halim, S.A. Short, J.A. Scott, R. Amal, G. Low, Modelling the leaching of Pb, Cd, As, and Cr from cementitious waste using PHREEQC, Journal of Hazardous Materials A215 (2005) 45–61.
- [13] L. De Windt, R. Badreddine, Modeling of long-term dynamic leaching tests applied to solidified/stabilised waste, Waste Management 27 (2007) 1638–1647.
- [14] J.V. Bothe Jr., P.W. Brown, Phreeqc modeling of Friedel's salt equilibria at 23 °C, Cement and Concrete Research 34 (2004) 1057–1063.
- [15] W. Hummel, U. Berner, E. Curti, F.J. Person, T. Thoenen, Nagra/PSI Chemical Thermodynamic Data Base 01/01, Universal Publishers, 2002.
- [16] LLNL Database Supplied with Phreeqc.
- [17] F. Ziegler, C.A. Johnson, The solubility of calcium zincate ($\text{CaZn}_2(\text{OH})_6 \cdot 2\text{H}_2\text{O}$), Cement and Concrete Research 31 (2001) 1327–1332.
- [18] A. Capmas, D. Ménérier-Sorrentino, The effect of temperature on the hydration of calcium aluminate cement, UITECR'89, 1989, pp. 1157–1170, cited by [14].
- [19] B. Lothenbach, F. Winnefeld, Thermodynamic modelling of the hydration of Portland cement, Cement and Concrete Research 36 (2006) 209–226.
- [20] L.O. Hoglund, K. Konsult, Project SAFE. Modelling of Long Term Concrete Degradation Processes in the Swedish SFR Repository, 2001 ISSN 1408-3091, SKB report R.01.08 SKB (<http://www.skb.se/upload/publications/pdf/R-01-08webb.pdf> consulted on 2009.04.16).
- [21] D. Damidot, F.P. Glasser, Thermodynamic investigation of the $\text{CaO-Al}_2\text{O}_3\text{-CaSO}_4\text{-H}_2\text{O}$ system at 50 and 85 °C, Cement and Concrete Research 22 (1992) 1179–1191.
- [22] E.J. Reardon, An ion interaction model for the determination of chemical equilibria in cement/water systems, Cement and Concrete Research 20 (1990) 175–192.
- [23] R.G. Perkins, C.D. Palmer, Solubility of chromate hydrocalumite ($3\text{CaO} \cdot \text{Al}_2\text{O}_3 \cdot \text{CaCrO}_4 \cdot x\text{H}_2\text{O}$), Cement and Concrete Research 31 (2001) 1741–1748.
- [24] F.P. Glasser, A. Kindness, S.A. Stronach, Stability and solubility relationships in AFm phases. Part I: chloride, sulphate and hydroxide, Cement and Concrete Research 29 (1999) 861–866.
- [25] T. Matschei, B. Lothenbach, F.P. Glasser, The AFm phase in Portland cement, Cement and Concrete Research 37 (2007) 118–130.
- [26] X.D. Li, Y.M. Zhang, C.S. Poon, I.M.C. Lo, Study of zinc in cementitious material stabilised/solidified wastes by sequential chemical extraction and microstructural analysis, Chemical Speciation and Bioavailability 13 (1) (2001).